THE ROYAL SOCIETY

Deflagrations, hot spots, and the transition to detonation

By Elaine S. Oran and Alexei M. Khokhlov

Laboratory for Computational Physics and Fluid Dynamics, Naval Research Laboratory, LCP&FD, Code 6404, Washington, DC, 20375, USA

A series of multidimensional numerical simulations were used to investigate how, through a series of shock–flame interactions, a turbulent flame may suddenly evolve into a detonation, the process of deflagration-to-detonation transition (DDT). The reactive Navier–Stokes equations were solved on an adaptive mesh that resolved selected features of the flow including the structure of the laminar flame. The chemical and thermophysical models used reproduced the flame and detonation properties of acetylene in air over a range of temperatures and pressures. The interactions of an incident shock with the initially laminar flame led to the formation of secondary shocks, rarefactions, and contact surfaces that continued to distort the flame surface, eventually creating a turbulent flame brush. Pressure fluctuations, generated by shock–flame interactions in the flame brush, were the seeds for hot spots in unreacted material. The simulations showed that these hot spots underwent transition to a detonation when the gradients in induction time in the hot spot allowed the formation of spontaneous waves. An unsuccessful explosion in hot spots formed a shock with a flame left behind it. As the strength of the initial incident shock was increased, the location of DDT shifted from outside the flame brush to inside the flame brush. The main features of the simulated DDT process show trends similar to those observed in experiments.

Keywords: shock–flame interactions; deflagration-to-detonation transition; hot spots; turbulent flames; explosions

1. Introduction

Recently, we have completed a series of computations that investigate how a turbulent flame may suddenly evolve into a detonation, the process of deflagration-to-detonation transition (DDT) (Khokhlov *et al*. 1999*a*, *b*; Khokhlov & Oran 1999). The process by which a laminar flame, through a series of flame and fluid instabilities, becomes a turbulent flame is at least qualitatively understood. The transformation of a turbulent flame into a detonation has been an outstanding problem in combustion theory. In this paper we bring together selected results of DDT computations and discuss the role of hot spots in the DDT process.

Hot spots are one important element of detonation initiation. Extensive work on the mechanisms by which a hot spot generates a detonation has been done by John Clarke and co-workers, who constructed a theoretical description of how hot spots may evolve into a detonation (Clarke 1989; Clarke & Singh 1989; Nikiforakis &

Clarke 1996). This understanding provides a basis for the work described here, which addresses the question of how hot spots and turbulent flame brushes are related, and how exactly they fit into the process of DDT.

Experiments have shown that DDT is an extremely complex process involving deflagrations, shocks and shock reflections, boundary layers and all of their interactions with each other (Babkin & Kozachenko 1960; Soloukhin 1961; Urtiew & Oppenheim 1966). Exactly how DDT occurs is not clear from experiments, and seems to vary from event to event. A series of DDT experiments in long enclosed channels containing hydrogen and oxygen (Urtiew & Oppenheim 1966) ignited the mixtures at one end of the tube, created an initially laminar flame that then accelerated, became turbulent, and eventually formed a turbulent flame brush. When DDT occurred, the turbulent flame speed was considerably less than the Chapman–Jouguet velocity (D_{CJ}) of a detonation in the unburned material, and DDT appeared as a sudden explosion in the vicinity of this flame brush. Two basic pictures of DDT were observed: sometimes it happened inside the flame brush; sometimes it occurred in the preheated compressed material between the leading shock wave and the flame brush.

DDT was also observed in reflected shock-tube experiments where a flame brush was created by shock–flame interactions (Scarinci & Thomas 1990; Scarinci *et al*. 1993; Thomas *et al*. 1997). In such experiments, a laminar flame is ignited by sparks at a distance from the reflecting wall. Then the flame interacts first with the incident shock and later with the shock reflected from the end wall. The experiments showed that shock–flame interactions distort the flame and rapidly create a flame brush that later may lead to a detonation. When DDT occurred, the turbulent flame speed was considerably less than D_{CJ}. Here we study DDT numerically by simulating the reflected shock-tube experiments described above and focusing in on appearance of hot spots in turbulent flames and the subsequent transition to a detonation.

2. Problem description

In the experiments on which the simulations are based (Scarinci & Thomas 1990; Scarinci *et al*. 1993), multiple spherical laminar flames are ignited simultaneously ahead of the incident shock. By the time the incident shock reaches the flames, they have expanded and are beginning to coalesce to form a single corrugated flame surface. The experiments found that three situations arose, depending on the Mach number M_{s} of the incident shock. For the lowest values of M_{s}, detonation did not occur within the time frame of the experiments; for intermediate values of M_{s}, a detonation originated in shocked compressed material in the region away from the deflagration itself; and for the highest values of M_{s}, detonation was initiated more quickly and in the region of the flame brush.

Figure 1 is a schematic illustrating the initial and boundary conditions for the simulations. We model a section of the shock tube of $0.32 \times 0.01\ \mathrm{m}^2$, using reflecting boundary conditions on the right, a zero-gradient outflow boundary on the left and symmetry (mirror) conditions on the upper and lower boundaries. We thus model half of one cylindrically expanding flame. A driven shock is initially placed 0.02 m from the left boundary. The velocity of the gas is set to zero everywhere ahead of the shock. Between the left boundary and the shock, there is a uniform flow with the post-shock parameters determined from the Rankine–Hugoniot conditions for

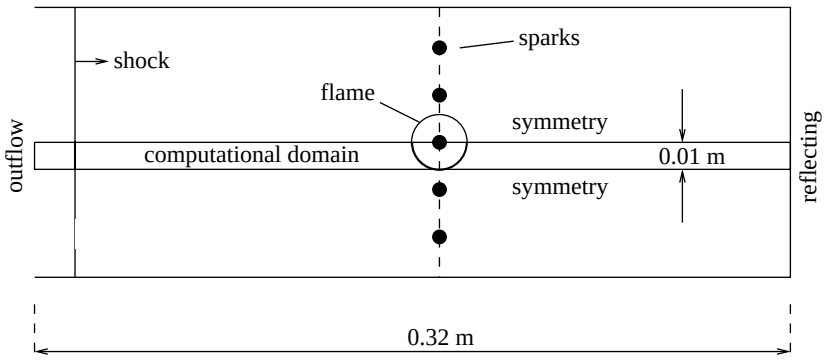

Figure 1. Schematic of the computational set-up.

a shock with a given Mach number, M_s. The left boundary condition provides a constant inflow of gas through this boundary until rarefaction and sound waves from the shock–flame interaction inside the computational domain reach the boundary. Thereafter, the inflow is modified by outgoing waves.

The computations solved the multidimensional time-dependent compressible reactive Navier–Stokes equations that include models for compressible fluid convection, chemical reactions and subsequent energy release, molecular diffusion, thermal conduction, and viscosity. The equations and the solution procedure are described in detail by Khokhlov *et al.* (1999*a*, *b*), who also provide information about the extensive series of resolution tests that have been performed. The flow was resolved to a scale less than the laminar flame thickness in regions in which there was a laminar flame by using a dynamically adapting mesh (Khokhlov 1998). This also ensured that shocks and incipient hot spots were well resolved. No subgrid model was used in the simulations, so that turbulence in the flow was produced self-consistently from flow interactions.

The simulations described in this paper are for a stoichiometric mixture of acetylene and air initially at $1.3158 \times 10^4\ \mathrm{N\,m^{-2}}$ (100 Torr) and 293 K. The chemical reactions were described by first-order Arrhenius kinetics expressed as

$$\frac{\mathrm{d}Y}{\mathrm{d}t} = -A\rho Y \exp(-Q/RT),$$

where Y is the mole fraction of reactant, $A = 1 \times 10^9\ \mathrm{m^3\,kg^{-1}\,s^{-1}}$ is the pre-exponential factor and $Q = 29.3RT_0$ is the activation energy. The reaction rate is proportional to the density ρ to account for the binary nature of chemical reactions taking place in real combustion systems. We assume that there is a similar temperature dependence for the kinematic viscosity, diffusion, and heat conduction, $\nu = \nu_0 T^n/\rho$, $D = D_0 T^n/\rho$ and $K/\rho C_p = \kappa_0 T^n/\rho$, where $\nu_0 = D_0 = \kappa_0 = 1.3 \times 10^{-6}$ are constants, $C_p = \gamma R/M(\gamma - 1)$ is the specific heat at constant pressure, $\gamma = 1.25$, and $n = 0.7$ emulates a typical temperature dependence of these coefficients in reactive hydrocarbon systems. The non-dimensional Lewis, Prandtl, and Schmidt numbers, $Le = K/\rho C_p D = \kappa_0/D_0$, $Pr = \rho C_p \nu/K = \nu_0/\kappa_0$ and $Sc = \nu/D = \nu_0/D_0$, are unity and independent of thermodynamic conditions. The properties of the chemical and thermophysical models, described in detail elsewhere (Khokhlov & Oran 1999), were such that the model gives the physically correct flame and detonation properties of this mixture over a range of temperatures and pressures. For this mixture,

the Chapman–Jouguet detonation velocity is $D_{\mathrm{CJ}} = 1870\,\mathrm{m\,s^{-1}}$, and the laminar burning velocity is $1.44\,\mathrm{m\,s^{-1}}$.

3. Shock-tube simulations

The interactions of an incident shock and an initially laminar flame created a multiplicity of secondary shocks and rarefactions, and eventually led to the formation of a turbulent flame brush. Studies of this type of interaction have been pioneered by Markstein (1964). In the simulations and experiments described here, the incident shock is a device to create a turbulent flame quickly. The composition, initial temperature and pressure of the unshocked gas were always the same, but the strength of the incident shock was varied.

The studies progressively increased the values of the Mach number of the incident shock, $M_{\mathrm{s}} = 1.4, 1.5, 1.63$. Computations were for both the two-dimensional problems described above, in which the shock hits an initially circular flame (described above), and for equivalent one-dimensional computations, in which the initial conditions correspond to the condition on the centreline of the two-dimensional flame. The results of these are summarized by the x–t diagrams for $M_{\mathrm{s}} = 1.5$ and 1.63 in figures 2 and 3, respectively. (The x–t diagrams for $M_{\mathrm{s}} = 1.4$ are not included here. These do not show a DDT event, but do show many of the same features of the higher-M_{s} cases.) As can be seen in the figures, the two-dimensional simulations show the same trends as observed in the experiments: for $M_{\mathrm{s}} = 1.4$, there was no detonation during the time frame of the simulations; for $M_{\mathrm{s}} = 1.5$, a detonation arose in the shock-heated and compressed material between the deflagration and the reflected shock; and for $M_{\mathrm{s}} = 1.63$, a detonation arose in the region of the flame brush. However, in the one-dimensional case, detonation only occurred for $M_{\mathrm{s}} = 1.63$ in the shock-heated material ahead of the flame brush.

As shown in figure 2*a*, the main sequence of events for the $M_{\mathrm{s}} = 1.5$ one-dimensional simulations proceeds as follows. A shock hits a flame that is propagating in a channel. The initial shock is transmitted through the flame, and a rarefaction moves backwards into the previously shocked unburned material. As the transmitted shock emerges from the other side of the flame, a reflected shock moves back through the flame. The incident shock finally hits the end wall, where it reflects and hits the flame again. Finally, this reflected shock emerges from the flame and eventually catches up with the first reflected shock. This merging of reflected shocks is followed by a series of other shock mergings, as a sequence of other weaker shocks emerges from the now turbulent flame.

An x–t diagram for the two-dimensional case is shown on figure 2*b*, where both vertical and horizontal axes are the same as shown in figure 2*a*. Here the initial shock–flame interaction distorts and increases the flame surface through a Richtmyer–Meshkov (RM) instability. This instability is the result of an impulsive acceleration of a perturbed density discontinuity by a shock wave. It is somewhat different from the Rayleigh–Taylor instability, in which the interface between two fluids of different density is subjected to continuous acceleration. When an incident shock moving through unburned material interacts with a curved flame, vorticity is generated and unburned material is driven into the burned region (Markstein 1964). In the current computations, the first shock–flame interaction drives a funnel of unburned material into the flame (Khokhlov *et al*. 1999*b*). Then the transmitted incident shock further

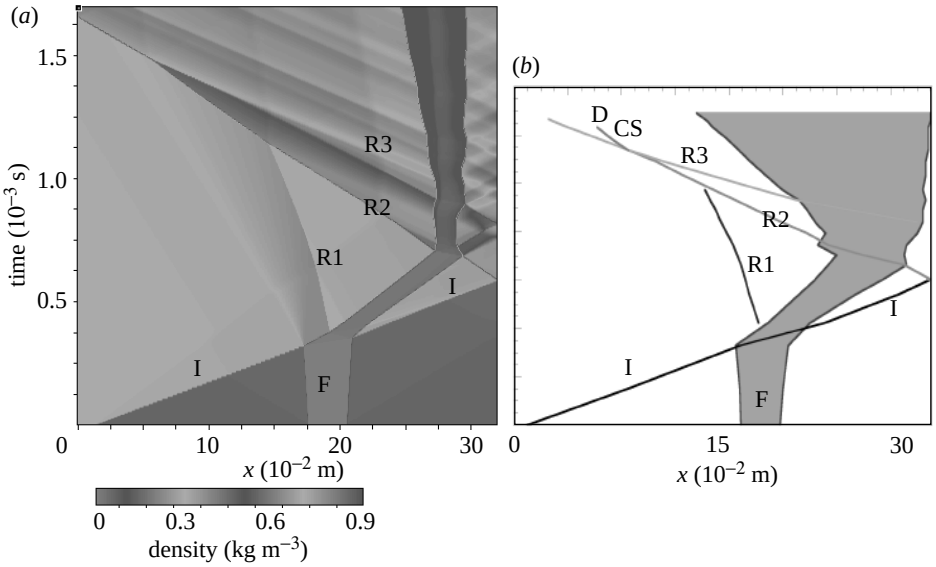

Figure 2. Space-time diagram for (*a*) one-dimensional computation with $M_s = 1.5$ incident shock (units on the scale are kg m^{-3}) and (*b*) two-dimensional computation, showing the location of the various fronts obtained from numerical simulations (see fig. 2 in Khokhlov *et al.* 1998*b*): I, incident shock; R1, first reflected shock; R2, second reflected shock; R3, third reflected shock; F, flame; CS, contact surface; D, detonation. The time-scales on the vertical axes are the same for both figures.

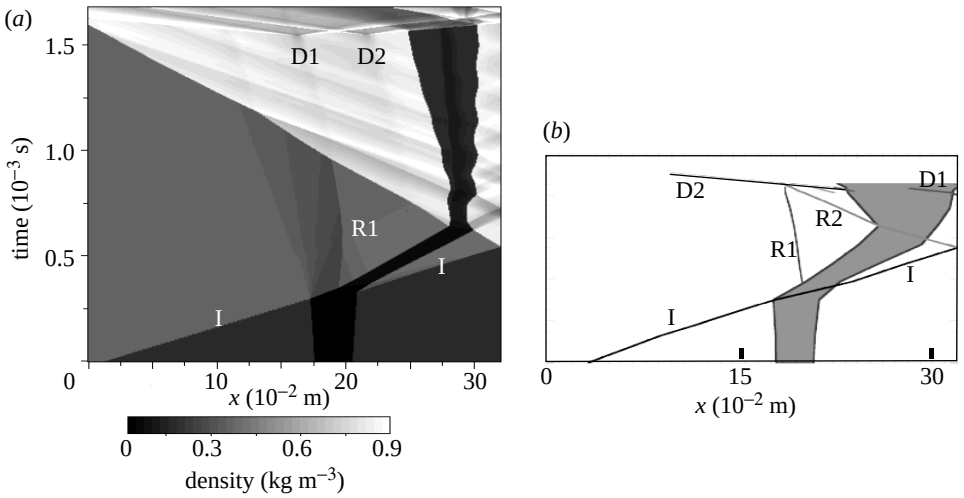

Figure 3. Space-time diagrams for (*a*) one-dimensional computation with $M_s = 1.63$ and (*b*) two-dimensional computation, where locations of the various fronts are taken from numerical simulations (see fig. 2 in Khokhlov & Oran 1999): I, incident shock; F, flame; R1, R2, R3, R4, various reflected shocks; D1, D2, detonations. The time-scales on the vertical axes are the same for both figures.

distorts the flame surface on the other side of the flame, this time pushing burned material into the unburned material to the right of the flame. Subsequent shocks continue to distort the flame surface, increase the rate at which the flame spreads, and enhance the rate of energy release. The difference in the extent of the flames in the one- and two-dimensional computations as a function of time is seen in figure 2.

The sequences in figure 3, for $M_s = 1.63$, are similar to $M_s = 1.5$ in the initial stages. The two-dimensional case is more compressed in time than the one-dimensional case. However, in the one-dimensional case in figure 3*a*, there are two hot-spot ignitions that lead to detonations, both of which are in the region between the reflected shock and the flame brush. In two dimensions, two detonation events are also visible, but the first is near the end wall and the other is in the flame brush.

In all cases, the presence of shocks has significant effects on the flame. The shocks heat and compress the material through which the flame must propagate, and this increases the energy-release rate. This increase in energy-release rate drives the shocks faster and increases the flame velocity. In the two-dimensional cases, there is the added affect of the RM and other instabilities that enhance the surface area of the flame, which has a significant effect on the rate of flame propagation.

Another phenomenon that should be mentioned is the effect of the turbulent flame on the unburned material. In all the simulations, even for the $M_s = 1.4$ case which did not detonate, the multiple shock–flame interactions in the turbulent flame generate fluctuations in pressure, temperature and density, and these propagate throughout the system. When these fluctuations become substantial in unburned material, they can create *hot spots*, or locations of enhanced reaction rate. An analysis of the computations showed that essentially no energy was released in the unburned material prior to onset of DDT (Khokhlov *et al*. 1999*b*). For higher M_s, these regions, or hot spots, can spontaneously ignite to create a detonation. Below we discuss how the conditions in these hot spots lead to detonation.

4. Discussion

(*a*) *Explosions in hot spots*

Here we consider the hot spots that arose in the two-dimensional simulations. In the $M_s = 1.5$ case, the detonation arose from hot spots in the heated, compressed material ahead of the flame brush. An analysis of the hot spots showed that their properties were not uniform, but they contained a gradient of induction time. Further analysis showed that the gradient was of the right magnitude to produce a supersonic spontaneous reaction wave that evolved into a detonation in the manner predicted by the Zeldovich gradient mechanism (Zeldovich *et al*. 1970).

Properties of the hot spot (marked as D in figure 2*b*) that led to the major detonation event for $M_s = 1.5$ are shown in figures 4 and 5. Figure 4 is a sequence of energy-release rate maps, density maps and density profiles showing the development of the spontaneous waves from two neighbouring hot spots in the brief interval between 1.2512 and 1.2529 ms. The earliest frame, 1.2512 ms, shows the hot spots located at the top and bottom of the domain. Figure 5*a*, which is also at 1.2512 ms, shows the distribution of τ_c, the chemical induction time, as computed by the Frank-Kamenetskii (1967) approximation. For the chemistry model used in the simulation, this estimate is accurate to 30% (Khokhlov *et al*. 1999*a*). There is a gradient of τ_c in each hot spot. The explosion begins in the location of minimum reaction time in the

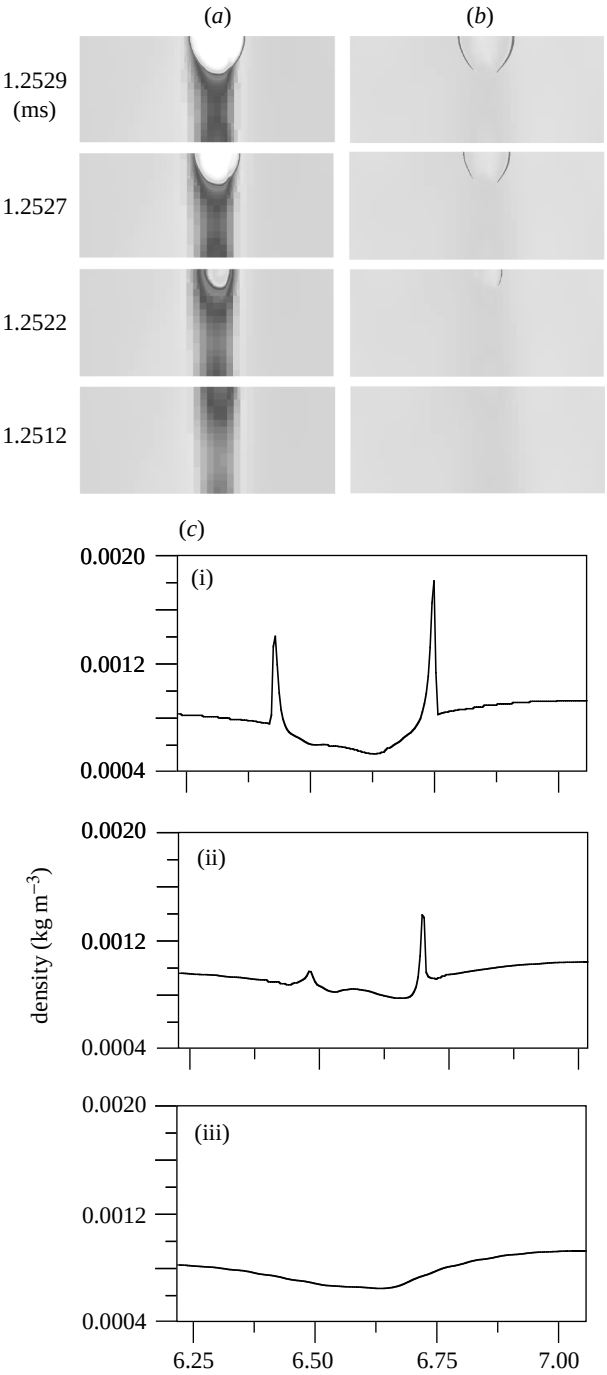

Figure 4. $M_s = 1.5$. Enlargement of the region of hot-spot ignition: (*a*) energy-release rate; (*b*) density. Dimensions of the regions shown are ($x = 0.053$–0.077 m, $y = 0.0$–0.01 m). (*c*) Density as a function of position ($y = 0.0073$ m) through the igniting hot spot shown at three later times are shown in (*a*) and (*b*): (i) 1.2529 ms; (ii) 1.2527 ms; (iii) 1.2522 ms.

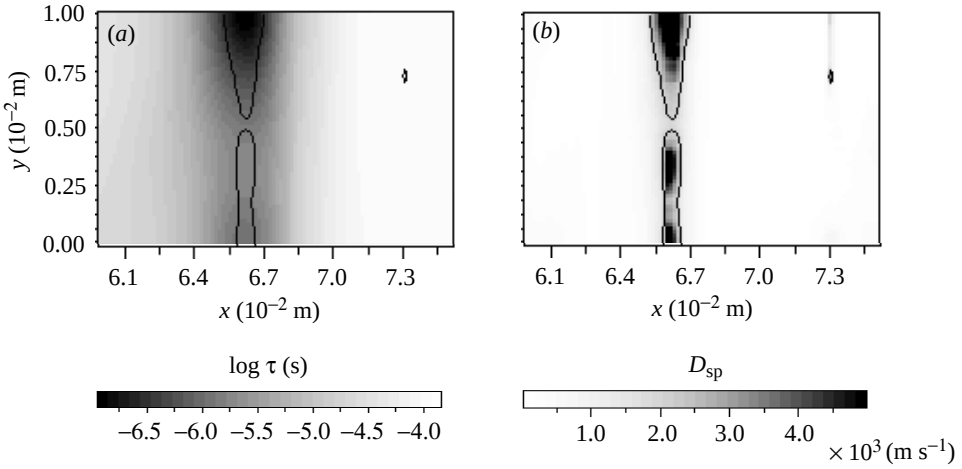

Figure 5. $M_s = 1.5$. Distribution of (a) chemical induction time τ_c and (b) the predicted spontaneous wave velocity D_{sp} for 1.2512 ms in figure 4.

upper hot spot, and propagates as a spontaneous wave with a speed $D_{sp} = |\nabla\tau_c|^{-1}$. Figure 5$b$ shows D_{sp} computed from τ_c. The values of D_{sp} are highest where $\nabla\tau_c$ is lowest. In the hot spots, $D_{sp} > D_{CJ}$. The contour $D_{sp} = D_{CJ}$ indicates the boundaries of the spontaneous flame region. The value of $D_{CJ} = 1.97\,\mathrm{km\,s^{-1}}$ is taken as the value in the precompressed and heated material of the hot spot ($T \simeq 780\,\mathrm{K}$, $P \simeq 1.64 \times 10^5\,\mathrm{N\,m^{-2}}$). The shape of the spontaneous region is not circular because the gradient is different in different directions.

At 1.2512 ms, no shock is present. However, the velocity of the spontaneous wave decreases as the reaction spreads at the initial stage of spontaneous wave propagation. When the velocity approaches D_{CJ}, a shock wave emerges and the spontaneous wave becomes a detonation. This transition does not occur simultaneously in all directions. The first appearance of the shock wave is on the right of the hot spot at 1.2522 ms, as seen on the density diagram. The transition occurs first where the gradient is the steepest. At 1.2529 ms, the reaction propagates downwards as a spontaneous wave and sideways as a detonation. The lower hot spot ignites later and proceeds through the same sequence of events.

Figure 4c shows density distributions along a horizontal line ($y = 0.0073$ m) passing through the hot spot at three times, 1.2522, 1.2527 and 1.2529 ms. At the earliest time, there are no shocks present. In the middle frame, a shock is propagating to the right and a spontaneous wave is moving to the left. The wave on the left is smooth, which is typical of spontaneous waves. By 1.2529 ms, the spontaneous waves have already made the transition to a detonation and two shocks are propagating in opposite directions.

For $M_s = 1.63$, two detonation events were observed: one near the end wall and another in the flame brush itself. An analysis of both of these events shows that both detonations occurred through the gradient mechanism. The transition at the end wall was qualitatively similar to the explosion observed for $M_s = 1.5$. However, the explosion in the flame brush occurred through an even more dynamic series of events than previously observed. Now the location of the transition was in a funnel of unreacted material that had been thrust into the flame brush as a result of the

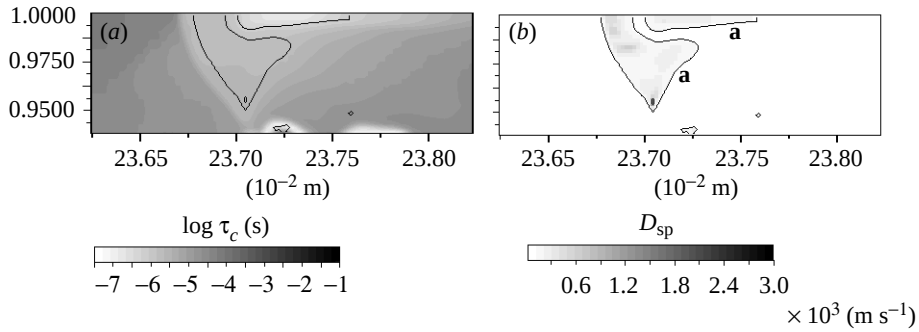

Figure 6. $M_s = 1.63$. An unsuccessful hot spot at 0.8576 ms: (*a*) chemical induction time; (*b*) spontaneous wave velocity. The contour **a** superimposed on both figures corresponds to $D_{sp} = 10^2$ m s^{-1}.

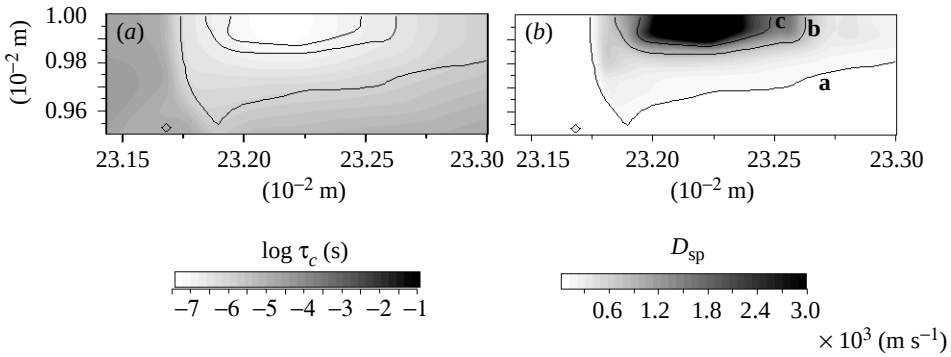

Figure 7. $M_s = 1.63$. A successful hot spot at 0.8660 ms: (*a*) chemical induction time; (*b*) spontaneous wave velocity. The contours **a**, **b** and **c** superimposed on both figures correspond to $D_{sp} = 10^2$, 10^3 and 2×10^3 m s^{-1}, respectively. Contour **c** is the contour of $D_{sp} = D_{CJ}$.

RM instability. Throughout the course of the creation of the flame brush and the distortion of the flame surface, this unreacted material had been shocked repeatedly. Because of the uneven corrugated surface of the flame in the funnel, the shocks passing through this interface create secondary shocks and generate instabilities. This can be viewed as somewhat similar to shocks passing through a channel with a rough wall. Thus many complex shock structures are formed, including oblique shocks, triple points and Mach stems.

The first hot spot to ignite in the funnel did not lead to a detonation, but to a shock and a flame. Figure 6 shows distributions of induction time and D_{sp} for this spot. The spontaneous velocity was much less than the sound speed, so that a supersonic spontaneous wave could not arise and a detonation did not form. However, the effect of this failed detonation was to further precondition the material around it. A second, nearby hot spot then exploded and generated a spontaneous wave that led to a detonation by the gradient mechanism. Figure 7 shows τ_c and D_{sp} maps and contours at one time, and figure 8 shows pressure maps and pressure contours

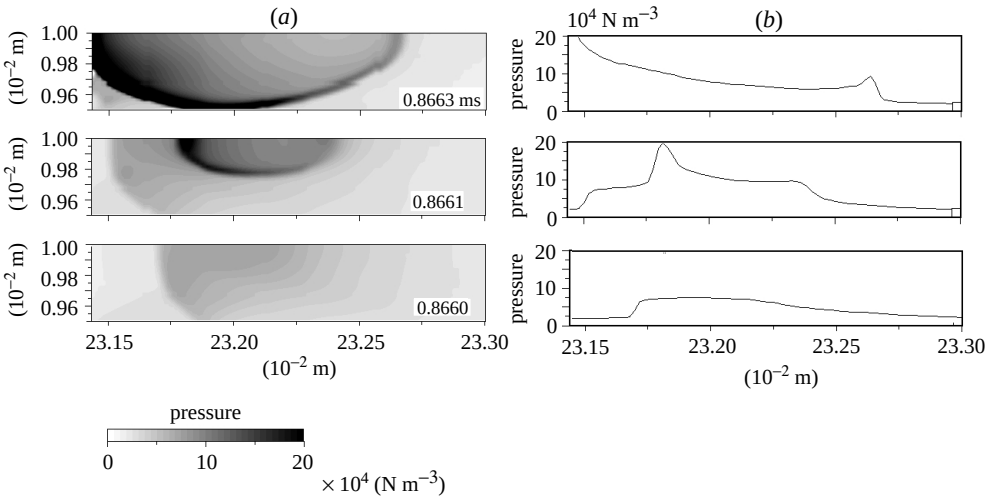

Figure 8. $M_s = 1.63$. Explosion of the successful hot spot shown in figure 10: (a) pressure distribution in the hot spot; (b) pressure profile through a horizontal cut at $y = 0.0099$ m.

through the successful hot spot at a sequence of times. There is a large region where $D_{sp} > D_{CJ}$, the existence of which made the initiation possible.

(b) *Dependence of the location of DDT on the strength of the incident shock*

The simulations show that increasing the value of M_s accelerates DDT and shifts the location of the hot spot that leads to detonation inside the flame brush. This can be explained by the decrease in induction time with increase in temperature. The funnel in the flame brush is the unreacted material that is subject to the most intense fluctuations. It is also strongly affected by the complex shock structures that move through it. Thus, if there is enough material in the funnel to contain a hot spot with conditions that could lead to a spontaneous wave, the funnel is a likely place for DDT to occur. When M_s is higher, the average temperature in the shocked, compressed material is higher. As a result, the size of the region of the induction-time gradient that can trigger a detonation becomes smaller. The small size of this region means that it can now be located inside the flame brush. When M_s is lower, the average temperature is lower, the gradient region must be larger and the funnel might not be large enough to contain the type of hot spot that could lead to detonation.

(c) *Dimensionality*

There were significant qualitative, as well as quantitative, differences between one- and two-dimensional calculations. Because of the added effects of the RM instability in creating a turbulent flame brush and maintaining it at an intense level of turbulence, it was easier to create conditions favourable for transition to detonation in the two-dimensional simulations. Detonations occurred more quickly, and the multidimensional nature of the flame meant that transition could actually occur in the flame brush itself.

The shape of the hot spot and the way the spontaneous wave propagated were different from case to case. However, the mechanisms of spontaneous wave propagation and transition are essentially one dimensional. Because of the supersonic nature of the spontaneous wave, the transition to detonation was independent along each ray of propagation. This supports the theoretical picture that the gradient mechanism is generic for DDT (Lee & Moen 1978).

Even though the computations were two dimensional and not three dimensional, they essentially showed the types of DDT events and of non-events observed at values of M_s that are very close to those used in the experiments. This agreement could be explained by the unsteady nature of the turbulence in the flame brush. Previously, by evaluating the effects of turbulent cascade versus the population of scales directly by RM, we have shown that the RM instability, which occurs in both two dimensions and three dimensions, is the major mechanism for populating turbulent scales (Khokhlov *et al*. 1999*b*). There we argued that it is even more important in three dimensions than in two dimensions. All scales, from the flame thickness to the large scale, are populated simultaneously by shock–flame interactions. Computations in three dimensions (reported later) show a similar picture of DDT.

(*d*) *Flamelets versus distributed flames*

In a previous paper (Khokhlov *et al*. 1997) we presented a theory for DDT that was applicable to situations in which there is no significant physical confinement or obstacles in the flow. In such situations, the only way to create a region in which there is a gradient of induction time capable of generating a spontaneous wave is to extinguish the deflagration to the point where hot burned material mixes well enough with unreacted material. We speculated there that for this mixing to happen, the flame has to be in the distributed regime. Then the occurrence of DDT would depend on two major factors: the strength of the turbulence and the combustion (flame and detonation) characteristics of the material. The important point is that the turbulence has to be able to break up and (at least partly) extinguish the flame.

In contrast to the unconfined situation, all three confined-shock-tube simulations described above show no evidence of the existence of a distributed flame. The computed flame surface was extremely resistant to being broken or extinguished. DDT occurred by the gradient mechanism, but in hot spots in preheated compressed unreacted material. We might have expected to find more distributed flames in the flame brush, but the little that was seen did not last long enough to affect the result. This result might be general, it might be the effect of some property of the chemical model used (such as $Le = 1$ or the fact that it is a one-step model and the details of the constituent species are not accounted for), or it might be due to the fact that radiation losses were neglected.

We believe that the basic principles needed to describe the two different situations, unconfined and confined, may be used to describe intermediate situations. For DDT to occur in the jet initiation experiments (Knystautas *et al*. 1978; Carnasciali *et al*. 1991; Dorofeev *et al*. 1993), in which a jet of turbulent, fully reacted (and therefore hot) material is injected into cold premixed gases, the turbulence should be of the right scale (strength and size) to mix enough hot and cold material to create the gradient of composition and temperature that would lead to DDT. Weak shocks, generated by unsuccessful hot-spot explosions, could help prepare the medium for DDT. Such speculations should be tested on a case-by-case basis.

5. Conclusions

The interactions of shocks and flames are important in creating the right conditions for DDT to occur. The shock–flame interactions, through the RM instability, are responsible for creating and maintaining a highly turbulent flame brush. We believe that the RM instability is the primary mechanism for generating turbulence in the brush in both two and three dimensions. The simulations have shown that the flow in and around the turbulent flame is extremely dynamic and complex. A study of the detailed density and pressure maps, as well as the integrated energy-release rates after the turbulent flame has developed, shows the presence of large fluctuations generated by interactions of weak shocks with the flame (Khokhlov *et al*. 1999*b*; Khokhlov & Oran 1999). This results in a complicated dynamic temperature distribution with many local maxima and minima. Some of these maxima, or hot spots, may autoignite and then lead to a detonation. An analysis of the hot spots that caused detonation showed that the transition to detonation occurred through the gradient mechanism.

There are two concepts of gas-phase DDT discussed in the literature. In one approach, DDT results from regions that have gradients in induction time (Zeldovich *et al*. 1970; Lee & Moen 1978). These gradients then allow spontaneous waves to arise, and these develop into a detonation. In the second approach, hot spots are caused by fluctuations in the material and, given the right conditions, a detonation occurs (Meyer & Oppenheim 1971). For the computations we have shown, these two approaches are not exclusive, but are consistent with each other. We have shown that the hot spots arise from fluctuations that increase as the turbulent flame becomes more intense. The mechanism by which a hot spot creates a detonation is by creating spontaneous waves that arise due to gradients of induction time.

The picture of DDT found in the simulations explains why DDT in the experiments is so sudden and why the location of DDT shifts into the region of the flame brush as the strength of the incident shock increases. Even though the simulations were for experiments in which the turbulent flame created a shock–flame interaction (Scarinci & Thomas 1990; Scarinci *et al*. 1993), we speculate that the mechanisms may be the same for DDT in accelerating flame in channels (Urtiew & Oppenheim 1966).

This work was sponsored by the Office of Naval Research and the NASA Astrophysical Theory Program. The authors are grateful to J. C. Clarke, G. Thomas, C. Sands, J. C. Wheeler, A. Chtchelkanova, K. N. C. Bray, C. Kaplan, N. Nikiforakis, and A. K. Oppenheim for many helpful discussions. This paper is declared a work of the US Government and is not subject to copyright protection in the United States.

References

Babkin, V. S. & Kozachenko, D. S. 1960 Development of detonation in rough tubes. *Zh. Prikl. Mek. Tek.* **3**, 163–174.

Carnasciali, F., Lee, J. H. S. & Knystautas, R. 1991 Turbulent jet initiation of detonation. *Combust. Flame* **84**, 170–180.

Clarke, J. F. 1989 Fast flames, waves, and detonation. *Prog. Energy Combust. Sci.* **15**, 241–271.

Clarke, J. F. & Singh, G. 1989 *A numerical simulation of shock-generated ignition using the random choice method*. Lecture Notes in Physics, vol. 351, pp. 22–35. Springer.

Dorofeev, S. B., Bezmelnitsin, A. V., Sidorov, V. P., Yankin, J. G. & Matsukov, I. D. 1993 Turbulent jet initiation of detonation in hydrogen–air mixture. In *14th Int. Coll. on Dynamics of Explosions and Reactive Systems*, vol. 2, pp. D2.4.1–D2.4.10.

Frank-Kamenetskii, D. A. 1967 *Diffusion and heat transfer in chemical kinetics*. Moscow: Nauka.

Khokhlov, A. M. 1998 Fully threaded tree for adaptive mesh fluid dynamics simulations. *J. Comp. Phys.* **143**, 519–543.

Khokhlov, A. M. & Oran, E. S. 1999 Numerical simulation of detonation initiation in a flame brush: the role of hot spots. *Combust. Flame* **119**, 400–416.

Khokhlov, A. M., Oran, E. S. & Wheeler, J. C. 1997 A theory of deflagration-to-detonation transition in unconfined flames. *Combust. Flame* **108**, 503–517.

Khokhlov, A. M., Oran, E. S., Chtchelkanova, A. Yu. & Wheeler, J. C. 1999*a* Interaction of a shock with a sinusoidally perturbed flame. *Combust. Flame* **117**, 99–116.

Khokhlov, A. M., Oran, E. S. & Thomas, G. O. 1999*b* Numerical simulation of deflagration-to-detonation transition: the role of shock–flame interactions in turbulent flames. *Combust. Flame* **117**, 323–339.

Knystautas, R., Lee, J. H. S., Moen, I. O. & Wagner, H. Gg. 1978 Direct initiation of spherical detonation by a hot turbulent gas jet. *Proc. 17th Int. Symp. on Combustion*, pp. 1235–1245. Pittsburgh, PA: The Combustion Institute.

Lee, J. H. S. & Moen, I. O. 1978 The mechanism of transition from deflagration to detonation. *Prog. Energy Combust. Sci.* **6**, 359–389.

Markstein, G. H. 1964 *Nonsteady flame propagation*, ch. D. New York: Macmillan.

Meyer, J. W. & Oppenheim, A. K. 1971 Coherence theory of the strong ignition limit. *Combust. Flame* **17**, 65–68.

Nikiforakis, N. & Clarke, J. F. 1996 Quasi-steady structures in the two-dimensional initiation of detonations. *Proc. R. Soc. Lond.* A **452**, 2023–2042.

Scarinci, T. & Thomas, G. O. 1990 Some experiments on shock–flame interaction. Preprint UCW/det905, Department of Physics, University of Wales, Aberystwyth.

Scarinci, T., Lee, J. H., Thomas, G. O., Bambrey, R. & Edwards, D. H. 1993 Amplification of a pressure wave by its passage through a flame front. *Prog. Astro. Aero.* **152**, 3–24.

Soloukhin, R. I. 1961 Transition from combustion to detonation in gases. *Zh. Prikl. Mek. Tek.* **4**, 128–132.

Thomas, G. O., Sands, C. J., Bambrey, R. J. & Jones, S. A. 1997 Experimental observations of the onset of turbulent combustion following a shock–flame interaction. In *Proc. 16th Int. Coll. on the Dynamics of Explosions and Reactive Systems*, pp. 2–5.

Urtiew, P. A. & Oppenheim, A. K. 1966 Experimental observation of the transition to detonation in explosive gas. *Proc. R. Soc. Lond.* A **295**, 13–38.

Zeldovich, Ya. B., Librovich, V. B., Makhviladze, G. M. & Sivashinsky, G. I. 1970 On the development of detonation in a nonuniformly heated gas. *Astronaut. Acta* **15**, 313–321.